

Design and off-design simulations of combined cycles for offshore oil and gas installations

Lars O. Nord*, Olav Bolland

Department of Energy and Process Engineering, Norwegian University of Science and Technology, Trondheim, Norway

Abstract

Combined cycles applied on offshore oil and gas installations could be an attractive technology on the Norwegian continental shelf to decrease costs related to CO₂ emissions. Current power plant technology prevailing on offshore oil- and gas installations is based on simple cycle gas turbines for both electrical and mechanical drive applications. Results based on process simulations showed that net plant efficiency improvements of 26–33% (10–13%-points) compared to simple cycle gas turbines can be achieved when the steam bottoming cycles are designed for compactness and flexibility. The emitted CO₂ could be decreased by 20–25% by opting for a combined cycle rather than a simple cycle gas turbine. A clear disadvantage for offshore applications is that the weight-to-power ratio was 60–70% higher for a compact combined cycle than for a simple cycle gas turbine based on results in this study. Once-through heat recovery steam generator technology can be an attractive option when designing a steam bottoming cycle for offshore applications. Its flexibility, the avoidance of steam drums, and, with the right material selection, the possibility to avoid the bypass stack while allowing for dry heat recovery steam generator operation are all advantages for offshore applications. All process models, that were developed for offshore installations in the study presented, included once-through technology. A combined cycle plant layout for an offshore installation with both mechanical drive and generator drive gas turbines was included in the study. This setup allows for flexibility related to changes in demand for both mechanical drive and electricity. With the selected setup, designed for 60 MW shaft power, demand swings of approximately ± 10 MW could be handled for either mechanical drive or electrical power while keeping the other drive-mode load constant.

Keywords: once-through, Rankine cycle, steam bottoming cycle, process simulation, steady-state

Nomenclature

A	heat transfer area (m ²)
D	diameter (m)

*Corresponding author
Email address: lars.nord@ntnu.no (Lars O. Nord)

H_f	fin height (m)
h	convective heat transfer coefficient ($\text{W}/\text{m}^2\cdot\text{K}$)
h_g	flue gas enthalpy (kJ/kg)
k	fluid thermal conductivity ($\text{W}/\text{m}\cdot\text{K}$)
LHV	lower heating value (kJ/kg)
m	mass (kg)
\dot{m}	mass flow (kg/s)
Nu	Nusselt number (-)
Pr	Prandtl number (-)
Q	heat duty (W)
R_f''	fouling factor ($\text{m}^2\cdot\text{K}/\text{W}$)
R_{rad}	radiation resistance (K/W)
R_{wall}	wall conduction resistance (K/W)
Re	Reynolds number (-)
RL_{gt}	relative gas turbine load (-)
T	temperature ($^{\circ}\text{C}$; K)
T_f	fin temperature (K)
T_g	gas temperature (K)
U	overall heat transfer coefficient ($\text{W}/\text{m}^2\cdot\text{K}$)
\dot{W}_{aux}	auxiliary power (W)
\dot{W}_{gt}	gas turbine gross power (W)
$\dot{W}_{net,elec}$	net electric power (W)
$\dot{W}_{net,plant}$	net plant power (W)
\dot{W}_{shaft}	shaft power (W)

\dot{W}_{st}	steam turbine gross power (W)
$w_{dry,loss}$	dry steam turbine exhaust losses (kJ/kg)
$w_{st,loss}$	steam turbine exhaust losses (kJ/kg)
x_m	mean step steam quality (-)
y	moisture content (-)
β	Baumann coefficient (-)
Δp	pressure loss (bar)
ΔT	temperature difference (K)
ΔT_{lm}	log mean temperature difference (K)
η_{dry}	dry step efficiency (-)
η_{gen}	generator efficiency (-)
$\eta_{net,plant}$	net plant efficiency (-)
η_o	overall surface efficiency (-)
$\eta_{Rankine}$	Rankine cycle efficiency (-)
η_{sc}	steam cycle gross efficiency (-)
η_{step}	corrected step efficiency (-)
χ_{hrsg}	heat recovery effectiveness (-)
DLE	dry low emission
GT	gas turbine
HRSG	heat recovery steam generator
OTSG	once-through heat recovery steam generator
ST	steam turbine

1. Introduction

There are CO₂ costs related to hydrocarbon use in the offshore industry on the Norwegian continental shelf. These costs are a combination of a CO₂ tax introduced by the Norwegian government in 1991 and the CO₂ quota system introduced in 2005. Since 2008, the quota system has been tied to the European CO₂ quota system. For the offshore industry, there is no free CO₂ quota allotted; instead the offshore industry has to buy its entire CO₂ quota. The CO₂ tax is related to fuel usage and not actual CO₂ emissions. In a white paper on climate efforts, which has been approved by the Norwegian parliament, an increase in the CO₂ tax is proposed [1]. In the long term, the CO₂ tax will be adjusted for fluctuations in the CO₂ quota market price to allow for an almost constant total cost per ton released CO₂. Based on [1], the CO₂ tax on emissions from Norway's offshore petroleum production will rise by approximately €25 per ton CO₂ released. This tax level would be nearly twice the 2012 tax level.

One of the goals of the increased CO₂ tax is to increase the focus on energy efficiency. One way of increasing the efficiency of the offshore power plants, and thereby decreasing the CO₂ cost per generated MW, is to add steam bottoming cycles to the current simple cycle gas turbines (GTs) that prevail offshore for mechanical drive and power generation. As a result of the 1991 CO₂ tax, combined cycles for the offshore industry were discussed and, to some extent, implemented in the 90s [e.g., see 2, 3, 4]. However, widespread use of steam bottoming cycles in the offshore sector has not, as of 2012, been implemented. Challenges include weight and size limitations, harsh conditions, and the need for treated feed and makeup water, as described in [5].

Offshore concepts, including combined cycles, with CO₂ capture have also been studied [6]. Marine combined cycles for ships is a related field with some commonalities with offshore applications, such as the need for compactness. The topic of marine combined cycles is discussed in [7].

This paper addresses design and off-design operation of combined cycles for offshore installations. The design of a combined cycle tailored towards an offshore installation requires a lower weight and volume compared to that of an onshore plant. Offshore installations are focused more on the oil and gas operations and less on the power plant necessary to supply electricity, heat, or mechanical drive to the processes. In a land-based power plant, the focus is usually on operating the plant as efficiently as possible for a given power demand. Offshore, the power plant has to adjust to whatever is needed for the oil and gas operations. This often leads to operation at off-design conditions.

Once-through heat recovery steam generator (OTSG) technology can be an attractive option when designing steam bottoming cycles for offshore installations. Its flexibility, the avoidance of steam drums, and, with the right material selection, the possibility to avoid the bypass stack while allowing for dry heat recovery steam generator (HRSG) operation are all advantages for offshore applications [8, 9]. A comparison between a drum-type HRSG and a once-through HRSG for offshore applications was performed in [5]. It

was concluded that a suitable HRSG design for offshore applications could be a single-pressure OTSG with a material selection of tubing and piping that allows for dry HRSG operation and thereby avoiding the bypass stack. Based on these conclusions, the focus of this paper is on single-pressure OTSG-based combined cycles, although, as a land-based reference plant, a dual-pressure drum-type HRSG system was analyzed. Also, since the prevailing technology offshore is based on simple cycle GTs, that setup was included for comparison.

The remainder of the article is divided into the following sections: a description of the process, model assumptions, and methodologies used are presented in Section 2. The results of the process simulations are presented in Section 3, and concluding remarks are given in Section 4.

2. Methodology

This section includes descriptions of the definitions, processes, and component models utilized both for design and off-design analyses. Off-design analysis investigates how the plant behaves when departure from the design point occurs. For the off-design cases presented in this paper, the focus was on plant behavior when the demanded power output (mechanical or electrical) of the plant changed.

GT PRO, GT MASTER, THERMOFLEX, and PEACE by Thermoflow Inc. were the software used for the combined cycle process modeling, process simulations, and weight estimations [10]. The unit operation models described in Sections 2.3–2.6 were included in the software. The IAPWS-IF97 water and steam properties were used [11].

2.1. Definitions

The gas turbine gross power output was defined as:

$$\dot{W}_{gt} = (\dot{W}_{shaft}\eta_{gen})_{gt} \quad (1)$$

where \dot{W}_{shaft} is the shaft power and η_{gen} is the generator efficiency. For an electrical drive application, \dot{W}_{gt} corresponds to the electrical output at the generator terminals. In a mechanical drive setup, η_{gen} would fall out.

The steam turbine gross power output was defined as:

$$\dot{W}_{st} = (\dot{W}_{shaft}\eta_{gen})_{st} \quad (2)$$

This is the electrical output at the steam turbine generator terminals.

The net plant power output was defined as:

$$\dot{W}_{net,plant} = \dot{W}_{gt} + \dot{W}_{st} - \dot{W}_{aux} \quad (3)$$

where \dot{W}_{aux} is the auxiliary power requirement. Note that all the power terms were defined as their absolute values, meaning all terms were considered positive and the sign handled in the equation itself.

The net plant efficiency was defined as:

$$\eta_{net,plant} = \frac{\dot{W}_{net,plant}}{(\dot{m}LHV)_{ng}} \quad (4)$$

where \dot{m}_{ng} is the natural gas mass flow entering the system and LHV_{ng} the lower heating value of the natural gas.

The gross efficiency of the steam cycle was defined as:

$$\eta_{sc} = \chi_{hrsg} \cdot \eta_{Rankine} \quad (5)$$

where the heat recovery effectiveness, χ_{hrsg} , was defined as:

$$\chi_{hrsg} = \frac{h_{g,in} - h_{g,out}}{h_{g,in} - h_{g,amb}} \quad (6)$$

and the efficiency of the Rankine cycle, $\eta_{Rankine}$, was defined as:

$$\eta_{Rankine} = \frac{\dot{W}_{st}}{\dot{m}_g(h_{g,in} - h_{g,out})} \quad (7)$$

$h_{g,in}$ is the enthalpy of the flue gases at the inlet of the HRSG, $h_{g,out}$ the enthalpy of the flue gases at the outlet of the HRSG (stack), $h_{g,amb}$ the enthalpy of the flue gases at site ambient conditions, and \dot{m}_g the mass flow of the flue gases.

For the off-design analyses, part load operational points were based on relative gas turbine load:

$$RL_{gt} = \frac{\dot{W}_{gt}}{\dot{W}_{gt,d}} \quad (8)$$

$\dot{W}_{gt,d}$ is here the gas turbine gross power output at design conditions.

CO₂ emitted from the power plant was defined as:

$$CO_2 \text{ emitted} = \frac{\dot{m}_{CO_2}}{\dot{W}_{net,plant}} \quad (9)$$

where \dot{m}_{CO_2} is the mass flow of carbon dioxide emitted from the plant.

The weight-to-power-ratio of the plant was defined as:

$$Weight-to-power-ratio = \frac{m_{plant}}{\dot{W}_{net,plant}} \quad (10)$$

where m_{plant} is the total mass of all the included components in the power plant. Included in the weight estimations were gas turbines with auxiliaries, steam turbine, generators, condenser, heat recovery steam generator, stacks, pumps, water treatment system, and water tanks. The weight estimations were based on component weights and did not include detailed project engineering such as equipment layout, pipe runs, skid structure, etc. Therefore, an actual installation would include additional weight. For the steam cycle, the wet weight (i.e., including the H₂O in the system) was utilized.

2.2. Process description

Four different plant layouts were modeled and simulated. The layouts were selected to compare a combined cycle designed for an onshore plant, with a simple cycle GT (current dominating power generation technology for offshore applications), as well as with combined cycle technology designed for offshore installations. For the combined cycles tailored towards offshore applications, two separate layouts were modeled: a layout with one GT, one OTSG, and one ST, and a layout which could represent an offshore configuration where both mechanical drive and generator drive are needed. All layouts, described in a–d, were based on the same gas turbine technology:

- a) Combined cycle based on a GE LM2500+G4 (60 Hz) and a dual-pressure HRSG. This represents a combined cycle designed for an onshore plant and was used as a reference plant.
- b) Simple cycle GT. This represents the prevailing power generation technology offshore. Same GT as in layout a.
- c) Combined cycle with one GT, one single-pressure OTSG, and one ST. Same GT as in layout a.
- d) Combined cycle with one mechanical drive GT, one generator drive GT, one dual-inlet, single-pressure OTSG, and one ST. The generator drive GT was the same as in layout a, and the mechanical drive GT was chosen as the 6100 rpm version of the LM2500+G4, also called PGT25+G4 [12]. The steam cycle was designed for 70% relative GT load to allow for operational flexibility.

Layout a is schematically shown in Fig. 1 and a schematic of a combined cycle based on the setup described in d is shown in Fig. 2. The assumptions for the process models are listed in Table 1, and the selection of steam cycle parameters is shown in Table 2. The steam parameters for the combined cycles applied to offshore installations were selected with a focus on low weight rather than on high efficiency, as described in [5]. The combined cycle designed for an onshore installation did not have the tight requirements on space and weight and the design was therefore focused more on efficiency than on weight [5].

The electrical frequency was selected as 60 Hz. On the Norwegian offshore oil and gas projects there is a mixture of 50 Hz and 60 Hz installations. The majority of the installations are not connected to the onshore grid and can therefore have a different frequency than the electrical grid. The gas turbine models in GT PRO for the GE LM2500+G4 series were better for the 60 Hz models than for the 50 Hz models. The 50 Hz models in the GT PRO database were geared versions of the 60 Hz models and had a higher maximum error on the performance. It can be argued that layout a (onshore plant) should have a frequency of 50 Hz since it would be connected to the Norwegian electrical grid. However, to be able to use the same GT for all layouts, also the onshore plant was designed for 60 Hz frequency.

2.3. Gas turbine model

GT PRO built-in compressor and turbine maps relating corrected inlet air mass flow to compressor pressure ratio and efficiency were utilized. The combustion model was based on an atom balance calculation

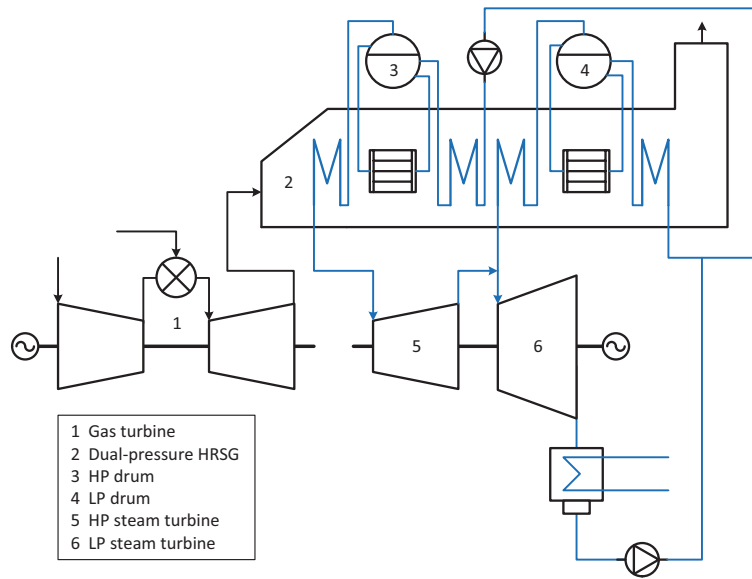


Figure 1: Layout of combined cycle for onshore installations with one gas turbine and one drum-type dual-pressure HRSG.

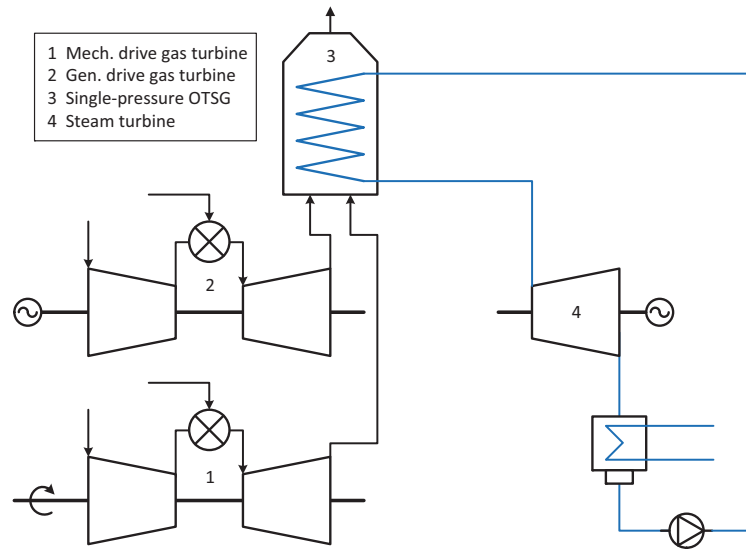


Figure 2: Layout of combined cycle for offshore oil and gas installations with two gas turbines and one dual-inlet once-through HRSG.

Table 1: Process model assumptions.

Site	
Ambient T ($^{\circ}\text{C}$)	15
Ambient pressure (bar)	1.013
Ambient relative humidity (%)	60
Frequency (Hz)	60
Cooling water system	direct water cooling
Cooling water	sea water
Cooling water T ($^{\circ}\text{C}$)	10
Cooling water ΔT (K)	10
Gas turbine	
Model type	GE LM2500+G4
GT fuel	methane
Lower heating value (kJ/kg)	50047
GT inlet Δp (bar)	0.010

Table 2: Selection of steam cycle parameters.

Cycle type	single-pressure OTSG	dual-pressure HRSG
Pressure levels HP/LP (bar)	25/-	55/7
Steam T HP/LP ($^{\circ}\text{C}$)	450/-	510/258
Pinch point ΔT HP/LP (K)	25/-	8/8
Condenser pressure (bar)	0.07	0.04
GT exhaust+HRSG Δp_{gas} (bar)	0.030	0.025

where it was assumed that the fuel was fully oxidized. Pressure drops for inlet air filter, ductwork, combustor, GT exhaust, and HRSG were taken into account.

The LM2500+G4 compressor is equipped with variable guide vanes with a set schedule, which affect the combined cycle performance (due to changes in the flue gas mass flow and temperature). Some of these compressor aspects, for the LM2500+, are described in [13].

For NO_x and CO considerations, the dry low emission (DLE) setup in the LM2500+G4 involves fuel staging in order to operate within the narrow flame temperature window [14]. This means, that different operating modes are active at different load points. Within each mode, the flame temperature will range between its maximum value for NO_x emissions and its minimum for CO emissions or flame blowout. Because of the different operating modes, the turbine exhaust temperature will vary up or down with decreasing load. This, in turn, affects the steam cycle, as shown in Section 3.

2.4. HRSG model

The control mode for the steam cycle was based on sliding pressure operation down to 75% of the design pressure. This pressure was reached at about 50% relative GT load. Below this threshold, throttle control was employed.

The HRSG temperature profile was calculated from its heat balance followed by calculation of the log mean temperature difference, ΔT_{lm} , and the corresponding UA parameter according to:

$$Q = UA\Delta T_{lm} \quad (11)$$

In the off-design scenarios the overall heat transfer coefficient U in the heat exchangers will vary. With inclusion of gas-side and water-side convection, tube material conduction, gas side radiation, as well as surface fouling and fin effects (extended surface), U can be calculated based on:

$$\frac{1}{UA} = \frac{1}{(\eta_o hA)_w} + \frac{R''_{f,w}}{(\eta_o A)_w} + R_{wall} + \frac{R''_{f,g}}{(\eta_o A)_g} + \frac{1}{(\eta_o hA)_g} + R_{rad} \quad (12)$$

R_{rad} is the radiation resistance, R_{wall} the wall conduction resistance, and R''_f the fouling factor. η_o is the overall surface efficiency of a finned surface and A is the heat transfer area. Subscripts w and g refer to the water- and gas-side of the heat exchanger, respectively.

Using the Nusselt number, the convective heat transfer coefficient h can be calculated:

$$Nu_D \equiv \frac{hD}{k} \quad (13)$$

D is the diameter and k the fluid thermal conductivity.

Gas-side heat transfer convective correlations were based on ESCOA[®] [15]:

$$Nu_D = C_1 C_3 C_5 Re Pr^{1/3} \left(\frac{T_g}{T_f} \right)^{1/4} \left(\frac{D + 2H_f}{D} \right)^{1/2} \quad (14)$$

The relations for factors $C_1 - C_5$ can be found in [16]. Re is the Reynolds number, Pr the Prandtl number, T_g the gas temperature, T_f the fin temperature, and H_f the fin height.

Water-side convective heat transfer correlations were based on:

$$Nu_D = 0.023Re^{4/5}Pr^{1/3} \quad (15)$$

Changes in pressure drops on both gas- and water-side were considered when operating at off-design conditions.

2.5. Steam turbine model

The steam turbine inlet has near constant volume flow throughout the operating range. This means that the ST velocity vectors are very similar at different load points leading to a near constant polytropic efficiency for the steam turbine. However, at low part load points, where throttling of the steam occurs, valve losses will increase. Also, the exhaust losses from the ST change at different load points.

The steam turbine efficiency was calculated by the method explained in [17]. The efficiency of each step within a particular steam turbine section was considered the same in the absence of steam moisture. This efficiency is defined as the dry step efficiency. To correct for condensing moisture entrained with the steam, the efficiency of a step with wet steam is reduced in proportion to the average moisture present within that step. The Wilson line represents the steam equilibrium quality at the onset of condensation within the steam turbine. Because of the high velocity and rapid cooling of the steam, it becomes supersaturated before liquid droplets actually begin to form. The selected definition of the Wilson line is that it corresponds to an equilibrium quality of 0.97. All steps whose exit quality is below the Wilson line have their efficiency corrected as follows:

$$\eta_{step} = \eta_{dry} - \beta(1 - x_m) \quad (16)$$

where η_{step} is the corrected step efficiency, η_{dry} the dry step efficiency, x_m the mean step steam quality, and β the Baumann coefficient. The Baumann coefficient was set to 0.72.

Dry exhaust loss is a function of the annulus velocity in the steam turbine exhaust. Further, the exhaust loss was corrected for wetness according to [17]:

$$w_{st,loss} = w_{dry,loss} \cdot 0.87(1 - y)(1 - 0.65y) \quad (17)$$

where $w_{st,loss}$ is the exhaust losses (kJ/kg) corrected for wetness, $w_{dry,loss}$ the dry exhaust losses, and y the moisture content ($1 - x$).

2.6. Condenser, cooling water pumps, and feedwater pumps

A direct seawater cooled condenser was modeled. The overall heat transfer coefficient was computed by including internal convection, tube wall conduction, fouling, and external condensation. The heat transfer coefficient was varied at off-design conditions.

Table 3: Comparison of simple cycle and combined cycle gas turbine plants: Process simulations in GT PRO versus 2012 Gas Turbine World Handbook (GTW).

Plant type	simple cycle	simple cycle	combined cycle	combined cycle
Source	GTW	GT PRO	GTW	GT PRO
Gas turbine	GE LM2500+G4	GE LM2500+G4	GE LM2500+G4	GE LM2500+G4
Frequency (Hz)	60	60	60	60
NO _x abatement	DLE	DLE	DLE	DLE
Net plant power output (MW)	not reported	32.2	45.7	45.3
GT gross power output (MW)	33.2	32.5	33.2	32.1
ST gross power output (MW)	-	-	13.4	13.7
Plant efficiency ^a (%)	38.9	38.6	53.6	53.8
GT exhaust mass flow (kg/s)	91.2	89.9	not reported	89.9
GT exhaust T (°C)	525	528	not reported	532

^agross for simple cycle; net for combined cycle

The cooling water pumps were considered to operate at the design point even during plant part load operation. This led to lower condensing pressure at part load operation.

Pump curves relating mass flow to head and efficiency were utilized for the feedwater pumps.

3. Results and discussion

3.1. Model validation

The 2012 Gas Turbine World Handbook (GTW) was used to validate the modeled dual-pressure HRSG reference combined cycle plant (layout a) [18]. Based on the combined cycle numbers presented in Table 3, the difference in GT power output was 3.3%, in ST power output, 2.2%, and in net plant efficiency, 0.4% when using the GTW values as basis for the comparison. Based on the simple cycle data (layout b), the exhaust temperature differed by 3 °C and the exhaust mass flow, by 1.4%.

The Oseberg combined cycle described in [4] was modeled in GT PRO for modeling calibration purposes. The model led to simulation results within 0.1% of the Oseberg documented steam turbine power output, while matching the live steam pressure and temperature. The Oseberg process model is further described in [5]. This calibration was performed to assure that the methods, tools, and assumptions used for the modeling of combined cycles for offshore installations were valid (layouts c and d).

The simulation results were deemed to be in satisfactory agreement with the validation data.

Table 4: Comparison of the four layouts described in Section 2.2 at steam cycle design conditions.

Plant layout		a	b	c	d
GT gross power output	\dot{W}_{gt} (MW)	32.1	32.5	32.1	46.1
ST gross power output	\dot{W}_{st} (MW)	13.7	-	11.3	19.9
Net plant power output	$\dot{W}_{net,plant}$ (MW)	45.3	32.2	42.9	64.4
Weight-to-power ratio	$m_{plant}/\dot{W}_{net,plant}$ (ton/MW)	~16	~7	~11	~12
Net plant efficiency	$\eta_{net,plant}$ (%)	53.8	38.3	51.0	48.2
CO ₂ emitted	$\dot{m}_{CO_2}/\dot{W}_{net,plant}$ (g/kWh)	367	516	387	409

3.2. Design conditions

Table 4 displays results for the four plant layouts, as described in Section 2.2. For layout d, the steam cycle was designed for 70% GT load for added power plant flexibility. The GT load could then be varied $\pm 30\%$ -points while staying within a 40–100% load range.

As expected, the simple cycle GT (layout b) has the lowest weight-to-power ratio, the lowest efficiency, and the highest CO₂ emitted. By adding a steam bottoming cycle as in layout c, an increase in efficiency of 33% can be achieved and the corresponding decrease in CO₂ emitted. Layout d with one mechanical drive GT and one generator drive GT has added flexibility compared to layout c, and could be an alternative for offshore applications where both mechanical drives and electricity are needed. Recall that the steam cycle, within the setup with two GTs and a dual-inlet OTSG, was designed for 70% GT load. This led to a higher weight-to-power ratio than if designed for 100% GT load. If designing that setup for full GT load, the net plant power output would be 86 MW and the weight-to-power-ratio ~ 10 ton/MW. For comparison, the onshore reference plant a, based on a dual-pressure HRSG, had a weight-to-power ratio of ~ 16 ton/MW.

3.3. Off-design conditions

Off-design simulations of plant layouts c and d were conducted. Firstly, results from off-design simulations of plant layout c will be presented. Refer to Figs. 3–4 for the results based on this plant layout. Secondly, results for plant layout d are discussed; refer to Table 5.

When comparing the T-Q diagrams for the 100% relative GT load case and the 60% GT load case, as shown in Fig. 3, the relative portion of economizing and superheating changed. At the 100% load point, 26% of the heat transferred from the flue gases to the water/steam in the HRSG was for economizing, whereas 17% of the heat transfer was for superheating. At the 60% load point, this shifted to 24% of the heat transferred for economizing and 20% for superheating. Therefore, to maintain a constant steam

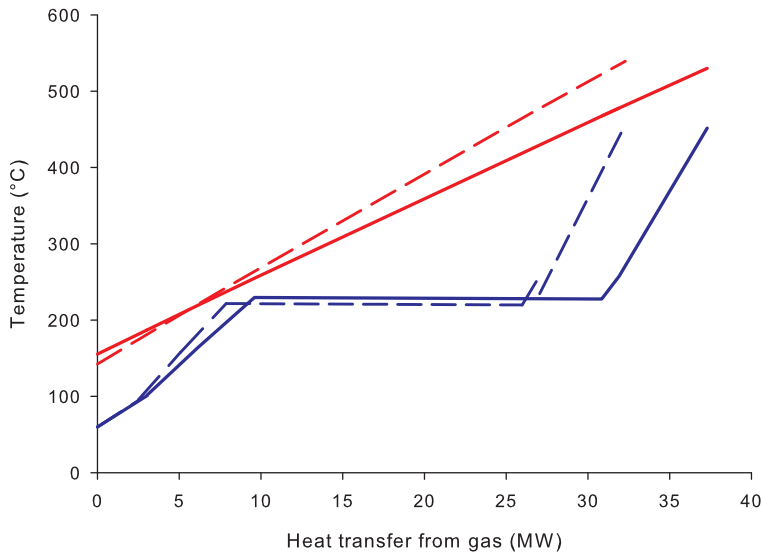


Figure 3: T-Q diagram at 100% and 60% GT relative load. Red, upper lines refer to HRSG flue gas; blue, lower lines to water/steam cycle. Dashed lines are for 60% GT relative load.

temperature supplied to the ST, desuperheating was necessary at part load. The desuperheating before the final superheating is evident in Fig. 3. Desuperheating after the HRSG was also utilized.

As described in Section 2.3, the LM2500+G4 dry low emissions combustion process is based on fuel staging, which affects the exhaust temperature. This is shown in Fig. 4 where one of the curves depicts the relative GT exhaust temperature (relative to design exhaust temperature in K) as a function of relative GT load. This, in turn, affects the steam cycle efficiency, where changes in the slope of the curve are a result of the fuel staging. A close resemblance between the relative exhaust temperature curve and the steam cycle efficiency is evident in Fig. 4.

Fig. 4 also indicates that after about 50% relative GT load, the combined cycle efficiency drops off steeply. This means that it might not be a good idea for prolonged operation at gas turbine loads below 50%. This corresponds to a combined cycle gross relative load of around 60%. At relative GT loads above 85%, the combined cycle efficiency can be kept at a value close to the design point.

Five scenarios based on plant layout d were simulated. The GTs both supplied heat to the dual-inlet OTSG. The steam cycle was designed for 70% GT load to allow for operational flexibility.

Scenario 1, as shown in Table 5, displays results for the steam cycle design point. Scenarios 2 and 3 are based on changes in demand for the mechanical drive GT. This could be due, for example, to changes in the gas compression power needed or changes in power to a water injection pump train. The mechanical drive GT was varied between 40% and 100% relative GT load. Further, the aim of scenarios 2 and 3 was to have a constant total electrical output from the generators coupled to the generator drive GT and the ST. This was accomplished by adjusting the electrical drive GT to compensate for changes in flue gas energy caused by

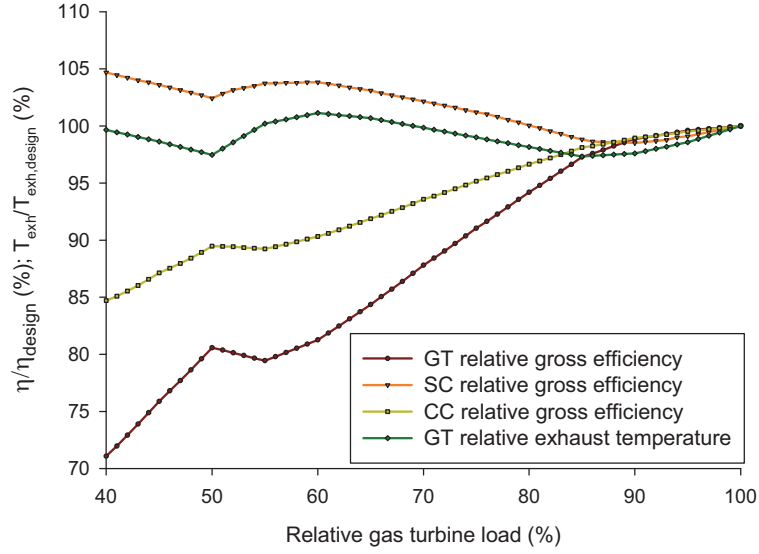


Figure 4: Relative GT exhaust temperature (based on K) and relative gross efficiencies of gas turbine, steam cycle, and combined cycle as a function of relative gas turbine load.

Table 5: Scenarios with results for plant layout d.

Scenario		1	2	3	4	5
GT _{mech} relative load	$RL_{gt,mech}$ (%)	70	100	40	70	70
GT _{gen} relative load	$RL_{gt,gen}$ (%)	70	67	75	40	100
ST gross power output	\dot{W}_{st} (MW)	19.9	20.8	18.4	17.9	21.1
Net elec. power output	$\dot{W}_{net,elec}$ (MW)	41.2	41.1	41.4	29.8	51.7
Net plant efficiency	$\eta_{net,plant}$ (%)	48.2	50.1	46.4	46.5	49.9
CO ₂ emitted	$\dot{m}_{CO_2}/\dot{W}_{net,plant}$ (g/kWh)	409	394	426	425	395

load changes of the mechanical drive GT. Scenarios 4 and 5 simulated the behavior if the electrical demand changed. The mechanical drive GT was here kept at the 70% load level.

The results, as presented in Table 5, show that with the selected setup, the electrical power can be altered ± 11 MW if operating the GT between 40% and 100% relative load. The mechanical drive power could be changed ± 9 MW. Further changes could be accomplished by allowing for lower GT load or by shutting down one GT or the steam cycle. Note the changes in net plant efficiency and emitted CO₂ for the different scenarios.

4. Conclusions

Combined cycles applied on offshore oil and gas installations could be an attractive technology on the Norwegian continental shelf to decrease costs related to CO₂ emissions. Net plant efficiency improvements of 26–33% (10–13%-points) compared to simple cycle gas turbines can be achieved when designing the steam bottoming cycles for compactness and flexibility. The emitted CO₂ could be decreased by 20–25% by opting for a combined cycle rather than a simple cycle GT. A clear disadvantage for offshore applications is that the weight-to-power ratio is 60–70% higher for a compact combined cycle than for a simple cycle GT.

Different scenarios related to the load for an offshore plant layout with both mechanical drive and generator drive GTs were included in the study. This setup allows for flexibility related to changes in demand for both mechanical drive and electricity. With the selected setup, designed for 60 MW shaft power, demand swings of approximately ± 10 MW could be handled for either mechanical drive or electrical power while keeping the other drive-mode load constant.

To justify installing a combined cycle on an offshore installation, a site specific techno-economic analysis should be performed. This was outside the scope of this study.

5. Acknowledgments

The authors are grateful for valuable comments received from the reviewers and editor. This publication forms a part of the EFFORT project, performed under the strategic Norwegian research program PETRO-MAKS. The authors acknowledge the partners Statoil, TOTAL E&P Norway, Shell Technology Norway, PETROBRAS, SINTEF Energy Research, NTNU-Norwegian University of Science and Technology, and the Research Council of Norway (203310/S60) for their support.

References

- [1] Ministry of the Environment, the Norwegian Government, Meld. St. 21 (2011–2012): white paper on climate efforts (2012).
- [2] S. A. Lloyd, Co-generation in offshore process platforms, in: 5th International Symposium and Exposition on Gas Turbines in Cogeneration, Repowering, and Peak-Load Power Generation; Budapest, Hungary, ASME IGTI Vol. 6, 1991, pp. 281–286.

- [3] R. Farmer, North Sea platforms are converting mech drives to comb cycle operation, *Gas Turbine World* November-December (1998) 12–16.
- [4] P. Kloster, Energy optimization on offshore installations with emphasis on offshore combined cycle plants, in: *Offshore Europe Conference*; Aberdeen, Scotland, Society of Petroleum Engineers Inc., 1999, paper no. SPE 56964.
- [5] L. O. Nord, O. Bolland, Steam bottoming cycles offshore—Challenges and possibilities, *Journal of Power Technology* 92 (3) (2012) 201–207.
- [6] Y. Bjerve, O. Bolland, Assessment of power generation concepts on oil platforms in conjunction with CO₂ removal, in: *Proceedings of the International Gas Turbine and Aeroengine Congress and Exposition*, American Society of Mechanical Engineers, 1994, pp. 1–5.
- [7] F. Haglind, A review on the use of gas and steam turbine combined cycles as prime movers for large ships. Part I: Background and design, *Energy Conversion and Management* 49 (12) (2008) 3458–3467.
- [8] M. F. Brady, Design aspects of once through systems for heat recovery steam generators for base load and cyclic operation, *Materials at High Temperatures* 18 (4) (2001) 223–229.
- [9] T. G. Koivu, New technique for steam injection (STIG) using once through steam generator heat recovery to improve operational flexibility and cost performance, in: *17th Symposium on Industrial Application of Gas Turbines (IAGT)*, Industrial Application of Gas Turbines Committee, 2007, pp. 1–32, paper no. 07-IAGT-2.2.
- [10] GT PRO, GT MASTER, THERMOFLEX, and PEACE Version 21, Thermoflow Inc., 2011.
- [11] W. Wagner, J. R. Cooper, A. Dittmann, J. Kijima, H. J. Kretzschmar, A. Kruse, R. Mareš, K. Oguchi, H. Sato, I. Stöcker, O. Šifner, Y. Takaishi, I. Tanishita, J. Trübenbach, T. Willkommen, The IAPWS industrial formulation 1997 for the thermodynamic properties of water and steam, *Journal of Engineering for Gas Turbines and Power* 122 (1) (2000) 150–180.
- [12] R. De Meo, M. D’Ercole, A. Russo, F. Gamberi, F. Gravame, D. Mucz, PGT25+G4 gas turbine development, validation and operating experience, Vol. 7 of *Proceedings of ASME Turbo Expo*, 2008, pp. 529–538, paper no. GT2008-50159.
- [13] A. R. Wadia, D. P. Wolf, F. G. Haaser, Aerodynamic design and testing of an axial flow compressor with pressure ratio of 23.3:1 for the LM2500+ gas turbine, *Journal of Turbomachinery* 124 (3) (2002) 331–340.
- [14] A. T. Evulet, GE Oil & Gas: Gas turbine combustion technologies, in: *CORE Symposium*, 2011, <http://www.coresymposium.com/2011CORE.html>.
- [15] ESCOA Fintube Manual, ESCOA Corp., Tulsa, OK, USA, 1979.
- [16] V. Ganapathy, *Industrial boilers and heat recovery steam generators*, Marcel Dekker, New York, USA, 2003, ISBN 0824708148.
- [17] R. C. Spencer, K. C. Cotton, C. N. Cannon, A method for predicting the performance of steam turbine generators 16,500 kW and larger, *Journal of Engineering for Power* 85 (4) (1963) 249–298.
- [18] *Gas Turbine World, GTW Handbook*, Vol. 29, Pequot Publishing Inc., Fairfield, CT, USA, 2012.